

# Human Herpesvirus-6 Reactivation, Mitochondrial Fragmentation, and the Coordination of Antiviral and Metabolic Phenotypes in Myalgic Encephalomyelitis/Chronic Fatigue Syndrome

Philipp Schreiner,\* Thomas Harrer,<sup>†</sup> Carmen Scheibenbogen,<sup>‡</sup> Stephanie Lamer,<sup>§</sup> Andreas Schlosser,<sup>§</sup> Robert K. Naviaux,<sup>¶</sup> and Bhupesh K. Prusty\*<sup>1</sup>

\*Lehrstuhl für Mikrobiologie, Julius-Maximilians Universität Würzburg, 97074 Würzburg, Germany; <sup>†</sup>Medizinische Klinik 3, Universitätsklinikum Erlangen, Friedrich-Alexander-Universität Erlangen-Nürnberg, 91054 Erlangen, Germany; <sup>‡</sup>Institut für Medizinische Immunologie, Charité-Universitätsmedizin Berlin, Campus Virchow-Klinikum, 13353 Berlin, Germany; <sup>§</sup>Rudolf-Virchow-Zentrum für Experimentelle Biomedizin, Julius-Maximilians Universität Würzburg, 97078 Würzburg, Germany; <sup>¶</sup>Department of Medicine, School of Medicine, University of California San Diego, San Diego, CA 92103; <sup>||</sup>Department of Pediatrics, School of Medicine, University of California San Diego, San Diego, CA 92103; and <sup>#</sup>Department of Pathology, School of Medicine, University of California San Diego, San Diego, CA 92103

## ABSTRACT

Myalgic encephalomyelitis/chronic fatigue syndrome (ME/CFS) is a multifactorial disorder with many possible triggers. Human herpesvirus (HHV)-6 and HHV-7 are two infectious triggers for which evidence has been growing. To understand possible causative role of HHV-6 in ME/CFS, metabolic and antiviral phenotypes of U2-OS cells were studied with and without chromosomally integrated HHV-6 and with or without virus reactivation using the histone deacetylase inhibitor trichostatin-A. Proteomic analysis was conducted by pulsed stable isotope labeling by amino acids in cell culture analysis. Antiviral properties that were induced by HHV-6 transactivation were studied in virus-naïve A549 cells challenged by infection with influenza-A (H1N1) or HSV-1. Mitochondria were fragmented and 1-carbon metabolism, dUTPase, and thymidylate synthase were strongly induced by HHV-6 reactivation, whereas superoxide dismutase 2 and proteins required for mitochondrial oxidation of fatty acid, amino acid, and glucose metabolism,

Received for publication January 21, 2020. Accepted for publication April 5, 2020.

**Address correspondence and reprint requests to:** Prof. Robert K. Naviaux or Dr. Bhupesh K. Prusty, University of California, San Diego, 214 Dickinson Street, Clinical Teaching Facility, Room C107, San Diego, CA 92103 (R.K.N.) or Department of Microbiology, Julius-Maximilians Universität Würzburg, 97074 Würzburg, Germany (B.K.P.). E-mail addresses: rnaviaux@health.ucsd.edu (R.K.N.) or bhupesh.prusty@uni-wuerzburg.de (B.K.P.)

ORCIDs: 0000-0002-1366-547X (P.S.); 0000-0003-0612-9932 (A.S.); 0000-0001-5832-2297 (R.K.N.); 0000-0001-7051-4670 (B.K.P.).

<sup>1</sup>Current address: Institute for Virology and Immunobiology, Julius-Maximilians-Universität Würzburg, Würzburg, Germany.

The proteomics data presented in this article have been submitted to the Proteomics Identifications Database (<https://www.ebi.ac.uk/pride/archive/projects/PXD016211>) under accession number PXD016211.

This work was supported in part by grants from The Solve ME/CFS Initiative (Ramsay Research Award) and HHV-6 Foundation (to B.K.P.) and gifts from the University of California San Diego Christini Fund, the Lennox Foundation, the JMS Fund, the Khosla Foundation, the Westreich Foundation, and the Malone Foundation (to R.K.N.), and grassroots support from over 2000 individuals who have each provided gifts in the past year to support Naviaux laboratory and Prusty laboratory research.

B.K.P. designed research; P.S., C.S., and B.K.P. performed research; C.S. and T.H. performed clinical analysis of patients and recruitment of patients; S.L. and A.S. performed mass spectrometry and data analysis; R.K.N. and B.K.P. analyzed the data; R.K.N., C.S., T.H., and B.K.P. wrote the manuscript.

**Abbreviations used in this article:** CDR, cell danger response; CFS, chronic fatigue syndrome; ciHHV-6, chromosomally integrated HHV-6; FISH, fluorescence in situ hybridization; HC, healthy control; HHV, human herpesvirus; iciHHV-6, genetically inherited ciHHV-6; IE, immediate early; ISG, IFN-stimulated gene; ME, myalgic encephalomyelitis; miRNA, microRNA; mitoGFP, mitochondrial GFP; MOI, multiplicity of infection; MS, mass spectrometry; MS/MS, tandem MS; PDP1, pyruvate dehydrogenase phosphatase catalytic subunit 1; 3p-hpRNA, triphosphate hairpin RNA; pSILAC, pulsed stable isotope labeling by amino acids in cell culture; qPCR, quantitative PCR; qRT-PCR, quantitative RT-PCR;  $\beta$ 2R,  $\beta$ 2 adrenergic receptor; ROS, reactive oxygen species; SIM, structured illumination microscopy; sncRNA-U14, small noncoding RNA-U14; SOD2, superoxide dismutase 2; TSA, trichostatin-A.

The online version of this article contains supplemental material.

This article is distributed under the terms of the [CC BY-NC-ND 4.0 Unported license](https://creativecommons.org/licenses/by-nc-nd/4.0/).

Copyright © 2020 The Authors

<https://doi.org/10.4049/immunohorizons.2000006>

ImmunoHorizons is published by The American Association of Immunologists, Inc.

including pyruvate dehydrogenase, were strongly inhibited. Adoptive transfer of U2-OS cell supernatants after reactivation of HHV-6A led to an antiviral state in A549 cells that prevented superinfection with influenza-A and HSV-1. Adoptive transfer of serum from 10 patients with ME/CFS produced a similar fragmentation of mitochondria and the associated antiviral state in the A549 cell assay. In conclusion, HHV-6 reactivation in ME/CFS patients activates a multisystem, proinflammatory, cell danger response that protects against certain RNA and DNA virus infections but comes at the cost of mitochondrial fragmentation and severely compromised energy metabolism. *ImmunoHorizons*, 2020, 4: 201–215.

## INTRODUCTION

Human herpesvirus (HHV)-6A and -6B are neurotropic viruses that carry stretches of telomeric repeats at both ends of their linear genome that facilitate their genome integration into human chromosomes to achieve latency (1). Chromosomally integrated HHV-6 (ciHHV-6) is at times genetically inherited (iciHHV-6) (2). Around 0.2–1% of humans carry iciHHV-6 (3), and 90–100% are infected by age 3 (4, 5). HHV-7 is another member of the betaherpesvirus family that shares similar genomic integration features with HHV-6 (6). HHV-6 and HHV-7 are frequently associated with several human diseases, including myalgic encephalomyelitis/chronic fatigue syndrome (ME/CFS) (7–9) that also involve mitochondrial dysfunction (10, 11). Mitochondrial dysfunction has long been predicted to play a crucial role in development and/or progression of ME/CFS. Alterations in mitochondrial dynamics, deficient mitochondrial ATP generation, and increased oxidative stress during ME/CFS have been reported (12, 13). Biophysical changes in cells from ME/CFS patients placed under osmotic stress have recently been used as an innovative diagnostic test for ME/CFS (14). However, the exact antecedent to mitochondrial modulation in ME/CFS is largely unknown. We have recently shown that HHV-6A reactivation induces mitochondrial fragmentation (15). In this study, we investigated potential infectious causes and molecular mechanism(s) behind mitochondrial dysfunction, likely resulting in the development and/or progression of ME/CFS, using HHV-6A reactivation as a model. Our results show a serum-transferrable innate immune activity in ME/CFS patients that induces a state of low mitochondrial activity accompanied by changes in mitochondrial dynamics that might contribute to disease pathophysiology.

## MATERIALS AND METHODS

### Cell culture and viral infection

A549 cells were purchased from American Type Culture Collection and were cultured in DMEM supplemented with 10% (v/v) FBS and 200 U/ml penicillin–streptomycin. U2-OS cells were grown in McCoy 5A Medium supplemented with 10% (v/v) FBS and 200 U/ml penicillin–streptomycin. Both of the cell lines were maintained at 37°C with 5% CO<sub>2</sub>. U2-OS cells carrying stable GFP expression within mitochondria were developed as mentioned before (16). U2-OS cells carrying latent HHV-6A is previously described (15).

For HSV-1 and influenza-A infection assays, A549 and U2-OS cells were seeded in six-well tissue culture plates for overnight. Culture supernatant was then replaced with fresh culture media and

patient serum in a ratio of 1:1. For culture supernatant-based adoptive transfer experiments, media were replaced with previously collected and sterile-filtered culture supernatants. After 48 h of incubation in the presence of serum containing media or previous culture supernatants, cells were washed twice with PBS and then infected either with influenza-A (A/Puerto Rico/8/1934 [H1N1]) or with wild-type HSV-1 (17+ strain) at a multiplicity of infection (MOI) of 1. One hour after viral infection, cells were again washed once with warm PBS and were allowed to grow further for another 24 h.

### Blood sample collection, DNA extraction, and quantitative PCR of HHV-6 and HHV-7 DNA

The blood samples were collected under written informed consent and the process was approved by the Ethikkommission of University of Würzburg. DNA extraction from total blood and PBMCs was carried out using QIAamp DNA Mini Kit (QIAGEN) following the manufacturer's protocol. DNA extraction from hair follicles was carried out using QuickExtract DNA Extraction Solution (Epicentre). Serum was isolated at the site of blood collection and was shipped to the laboratory for further analysis. Quantitative PCR (qPCR) assays for HHV-6 DNA (U94) and HHV-7 are previously described (17–19).

### RNA extraction and quantitative RT-PCR

Total cellular RNA extraction was carried using a Direct-zol RNA purification kit (Zymo Research) or TRI Reagent (Sigma-Aldrich). cDNA synthesis was carried out using Maxima First Strand cDNA Synthesis Kit (Thermo Fisher Scientific). qPCR was performed using SYBR Select Master Mix (Thermo Fisher Scientific) on a Roche LightCycler 96 System (Roche Life Science) using manufacturer's protocol and SYBR Green chemistry. Amplified data were analyzed using Roche LightCycler Software. As a positive control for activation of the viral RNA-sensing pathway and IFN-stimulated gene (ISG) response, cells were transfected with 0.1 ng of 5' triphosphate hairpin RNA (3p-hpRNA) (Invivogen) for 24 h using LyoVec (Invivogen) as a transfection reagent. The following primers were used for the real time PCR assays. HSV-1 ICP0\_1, 5'-ACTTTATCTGGACGGGCAAT-3'; HSV-1 ICP0\_2, 5'-GGTACGTAGTCTGCGTCGTC-3'; H1N1 ML\_1, 5'-GATCCCC GTTCCCATTAAGGG-3'; H1N1 ML\_2, 5'-GACCAATCCTGTC ACCTC-3'; HHV-6 U94\_1, 5'-GCGCTCCCGGTGAGTGATA-3'; HHV-6 U94\_2, 5'-AGGCCCATGGAGTGGGAGG-3'; HHV-6 P4L1, 5'-CCTGTTTTGATGCCAACGCA-3'; HHV-6 P4L2, 5'-AAAGCACGTTGTTGACGGTG-3'; IFN\_Beta\_1, 5'-AAACTAT GAGCAGTCTGCA-3'; IFN\_Beta\_2, 5'-AGGAGATCTTCAGTTT CGGAGG-3'; IFIT-1\_L1, 5'-ACAGCAACCATGAGTACAAATGG-3'; IFIT-1\_L2, 5'-CATCGTCATCAATGGATAACTCCC-3'; ICAM-1\_L1, 5'-CCACAGTCACCTATGGCAAC-3'; ICAM-1\_L2, 5'-TCTGG

CTTCGTCAGAATCAC-3'; 5S\_1, 5'-GTCTACGGCCATACCAC CC-3'; 5S\_2, 5'-AAAGCCTACAGCACCCGGT-3'; P115\_1, 5'-GGC GGAAGCGCTACATTTTCGCA-3'; P15\_2, 5'-TATTCATATTT GCTGCCGGTGGGA-3'.

#### **ATP assay**

To measure total ATP concentration in cells, Luminescent ATP Detection Assay Kit (Abcam) and ATP Determination Kit (Thermo Fisher Scientific) were used. Cells were grown in 96-well plates and were treated with the HHV-6 reactivating drug, trichostatin-A (TSA; 80 ng/ml) or solvent control (water). In parallel, similar experiments were carried out in which culture media were replaced with galactose (10 mM)-containing media 16 h prior to cell lysis. Luminescence measurement was carried out using an Infinite PRO multimode reader (Tecan). For adoptive transfer experiments, cells were grown in 48-well plates for 16 h. Afterwards sterile-filtered culture supernatants or serum samples were added to the cells and were allowed to grow for another 24 h. Cell lysates were prepared in PBS with 1% Triton X-100, and ATP measurement was carried out using Centro XS LB 960 Microplate Luminometer (Berthold Technologies).

#### **Mitochondrial microscopy and quantifications**

U2-OS cells expressing soluble GFP within mitochondria were developed using previously described protocols from our laboratory (16). Software and modified algorithm for mitochondrial surface area measurement using confocal and structured illumination microscopy (SIM) images were also previously described by us (16).

#### **Fluorescence in situ hybridization analysis**

Fluorescence in situ hybridization (FISH) to detect HHV-6A small noncoding RNA-U14 (sncRNA-U14) has been previously described by us (15).

#### **Cytokine analysis in PBMCs**

CFS patients were diagnosed at the Charité outpatient clinic for immunodeficiencies at the Institute for Medical Immunology. Diagnosis of CFS was based on Canadian Consensus Criteria and exclusion of other medical or neurologic diseases that may cause fatigue. Age- and sex-matched healthy controls (HC) were recruited from staff and did not suffer from fatigue. All patients and controls gave informed consent. The study was approved by the Ethics Committee of Charité University Medicine Berlin in accordance with the Declaration of Helsinki.

To assess monocyte cytokine production, 50  $\mu$ l of heparinized whole blood was added to 500  $\mu$ l of RPMI media with LPS (0.5 ng/ml; Milenia Biotec), and tubes were incubated for 4 h at 37°C and 5% CO<sub>2</sub>. To assess T lymphocyte cytokine production, 200  $\mu$ l of heparinized whole blood was added to 750  $\mu$ l of RPMI with ConA (50  $\mu$ g/ml; Sigma-Aldrich) and incubated for 24 h at 37°C and 5% CO<sub>2</sub>. Thereafter, tubes were centrifuged for 5 min at 1000  $\times$  g, and supernatant was collected and stored at -80°C until measurement. TNF- $\alpha$  and IL-1 $\beta$  were quantified in LPS-stimulated and Il-5 and IFN- $\gamma$  in ConA-stimulated samples by ELISA, according to manufacturer's instructions (BioLegend). The minimum detectable

concentration of the cytokines in this assay was 2 pg/ml (TNF- $\alpha$  and IL-5, respectively), 0.5 pg/ml (IL-1 $\beta$ ), or 4 pg/ml (IFN- $\gamma$ ). Twenty-two CFS patients and twenty-two HC patients were analyzed. Univariate statistical analysis of patients and HC groups was done using the Mann-Whitney *U* test. The *p* values are listed as \**p* < 0.05, \*\**p* < 0.01.

#### **Pulsed stable isotope labeling by amino acids in cell culture**

U2-OS cells were grown in McCoy 5A Medium containing 10% dialyzed FCS and light amino acids L-8662 ([<sup>12</sup>C]lysine; Sigma-Aldrich) and A-6969 ([<sup>12</sup>C]arginine; Sigma-Aldrich). Subsequently, solvent control-treated cells were grown in McCoy 5A Medium containing heavy isotope amino acids CNLM-291-H ([<sup>13</sup>C], [<sup>15</sup>N] lysine; Cambridge Isotope Laboratories) and CNLM-539-H ([<sup>13</sup>C], [<sup>15</sup>N]arginine; Cambridge Isotope Laboratories), whereas TSA-treated cells were grown in McCoy 5A Medium containing medium heavy amino acids DLM-2640 ([<sup>2</sup>H]lysine; Cambridge Isotope Laboratories) and CLM-2265-H ([<sup>13</sup>C]arginine; Cambridge Isotope Laboratories) for 48 h. Next, cells were lysed in lysis buffer (50 mM HEPES-NaOH [pH 7.5], 150 mM NaCl, 1% NP-40, 2.5 mM MgCl<sub>2</sub>, and protease inhibitor mixture). After incubation on ice for 10 min, cells were lysed using a 26-gauge needle followed by a mild water bath sonication to ensure complete nuclear lysis of the cells and centrifugation at 13,200 rpm for 20 min to remove cell debris. Heavy and medium pulse-labeled cell lysates were mixed in a 1:1 ratio, based on whole protein content estimated by a Bradford assay (500-0006; Bio-Rad Laboratories) before processing for mass spectrometry (MS).

#### **MS and MS data analysis**

MS analysis was carried out as previously described (20). Briefly, protein lysates were incubated in NuPAGE LDS sample buffer (Thermo Fisher Scientific) supplemented with 50 mM DTT, incubated for 10 min at 70°C, and alkylated by incubation with iodoacetamide (final concentration 120 mM) for 20 min at room temperature. Reduced and alkylated samples were loaded on NuPAGE Novex Bis-Tris 4–12% gradient gels (NP0321BOX; Thermo Fisher Scientific) and stained with Coomassie SimplyBlue (LC6060; Thermo Fisher Scientific). Whole lanes were cut into 15 bands. The bands were destained with 30% acetonitrile, shrunk with 100% acetonitrile, and dried in a vacuum concentrator. Digestion with 0.1  $\mu$ g of trypsin (V5280; Promega) per gel band was performed overnight at 37°C in 100 mM ammonium bicarbonate buffer. Peptides were extracted from the gel slices with 5% formic acid.

Nanoscale liquid chromatography –tandem mass (MS/MS) analyses were performed on an Orbitrap Fusion (Thermo Fisher Scientific) equipped with a PicoView Ion Source (New Objective) and coupled to an EASY-nLC 1000 (Thermo Fisher Scientific). Peptides were loaded on capillary columns (PicoFrit, 30 cm  $\times$  150  $\mu$ m ID; New Objective) self-packed with ReproSil-Pur 120 C18-AQ, 1.9  $\mu$ m (Dr. Maisch) and separated with a 45-min linear gradient from 3 to 30% acetonitrile and 0.1% formic acid and a flow rate of 500 nl/min. Both MS and MS/MS scans were acquired in the Orbitrap analyzer with a resolution of 60,000 for MS scans and

15,000 for MS/MS scans. Higher-energy collisional dissociation fragmentation with 35% normalized collision energy was applied. A top speed data-dependent MS/MS method with a fixed cycle time of 3 s was used. Dynamic exclusion was applied with a repeat count of 1 and an exclusion duration of 30 s; singly charged precursors were excluded from selection. Minimum signal threshold for precursor selection was set to 50,000. Predictive automatic gain control was used with automatic gain control as a target value of  $2e5$  for MS scans and  $5e4$  for MS/MS scans. EASY-IC was used for internal calibration.

For protein identification and quantification, MS raw data files were analyzed with MaxQuant version 1.6.2.2 (21), and database searches were performed with the integrated search engine Andromeda. The UniProt human reference proteome database and UniProt HHV-6A database were used in combination with a database containing common contaminants. The search was performed with tryptic cleavage specificity with three allowed miscleavages. Protein identification was under the control of the false-discovery rate ( $<1\%$  false-discovery rate on protein and peptide spectrum match level). In addition to MaxQuant default settings, the search was performed against the following variable modifications: protein N-terminal acetylation, glutamine to pyroglutamic acid formation, and oxidation (methionine). Carbamidomethyl (cysteine) was set as fixed modification.

For quantification of pulsed stable isotope labeling by amino acids in cell culture (pSILAC)-labeled proteins, the median was calculated from the  $\log_2$ -transformed normalized peptide ratios heavy to medium for each protein. Two ratio counts were required for protein quantification. Protein ratios were normalized for each experiment in intensity bins (at least 300 proteins per bin), and outliers were identified by boxplot statistics as significantly altered if their values were outside a  $1.5\times$  or  $3\times$  interquartile range (extreme outliers).

### Statistics

All statistical calculations were performed using GraphPad Prism 6.0. Error bars displayed on graphs represent the mean  $\pm$  SD of three or more independent replicates of an experiment. Statistical significance was calculated using a Student *t* test or one-way ANOVA followed by a Tukey multiple comparisons test. For image analysis, six or more biological replicates per sample condition were used to generate the representative data. qPCR, quantitative RT-PCR (qRT-PCR), and ATP assay data presented are representative of two to four independent experiments.

### Data accessibility

The MS proteomics data are available at ProteomeXchange Consortium via the PRIDE partner repository (<https://www.ebi.ac.uk/pride/archive/projects/PXD016211>) (22) with the dataset identifier PXD016211.

## RESULTS

### HHV-6A reactivation induces mitochondrial dysfunction

Various pathogenic infections alter mitochondrial dynamics and function for their own requirements. Viral infections, in particular,

target mitochondria to subvert innate immunity (23, 24). Hence, we suspected a viral cause behind development of ME/CFS, at least in a subset of patients. Using a unique *in vitro* model system in human U2-OS (bone osteosarcoma) cells, we have recently shown that HHV-6A transactivation induces mitochondrial fission, which is associated with altered host microRNA (miRNA) as well as the mRNA transcriptome (15). HHV-6 reactivation in U2-OS cells is nonproductive (15, 25) and is marked by initiation of transcription of several viral small noncoding RNAs in the absence of substantial viral DNA replication and viral protein synthesis (15). The viral polymerase is not detectable, and only a very few selective viral immediate early (IE) and early transcripts and proteins can be detected in these cells upon virus reactivation.

To further understand the potential effects of HHV-6A transactivation on mitochondrial function in U2-OS cells, we investigated changes in the host proteome upon virus reactivation in these cells. For this, HHV-6A reactivation was first induced using TSA, and mitochondrial fragmentation was documented using structured illumination microscopy (Fig. 1A). A predominant punctated form of mitochondria was observed upon HHV-6A reactivation (Fig. 1A). Using pSILAC-based quantitative proteomics, we observed an effect of virus reactivation on host cell protein dynamics. Data derived from two biological replicate experiments showed strong reproducibility of identification of proteins whose expression was altered upon viral reactivation (Supplemental Fig. 1A). We detected changes in expression dynamics of several key cellular proteins (Supplemental Fig. 1B). Because of our interest in HHV-6-mediated mitochondrial dysfunction, we further analyzed mitochondria-specific proteins. Several key mitochondrial proteins involved in glycolytic pathways, folic acid and 1-carbon metabolism, fatty acid oxidation, and amino acid metabolism were found to be altered upon HHV-6A transactivation (Fig. 1B), suggesting a potential effect on cellular as well as mitochondrial metabolism. The most interesting observation was the downregulation in expression of the mitochondrial proteins pyruvate dehydrogenase phosphatase catalytic subunit 1 (PDPI) and manganese-dependent superoxide dismutase 2 (SOD2). Increased oxidative stress (26), sometimes referred to as the oxidative shielding response (27), and altered pyruvate dehydrogenase functions (28) are key features of ME/CFS. Decreased SOD2 levels can contribute to increased reactive oxygen species (ROS) within the cell. In a previous study, we have shown increased ROS in HHV-6-infected cells (29). Hence, we speculated a direct role of HHV-6 infection in pathophysiology of ME/CFS.

To understand consequences of HHV-6-mediated mitochondrial alteration on host cell metabolism, we focused on increased mitochondrial fission in HHV-6-reactivated cells. Increased mitochondrial fission decreases the respiratory capacity of the cell (30), lowering cellular ATP production (31). Reciprocally, lower cellular energy levels can also induce mitochondrial fragmentation (reviewed in Ref. 32). Hence, we asked if HHV-6A transactivation also leads to lower ATP content in the cell. We measured the ATP contents of U2-OS cells in the presence or absence of latent HHV-6A (Fig. 1C). Furthermore, we reactivated

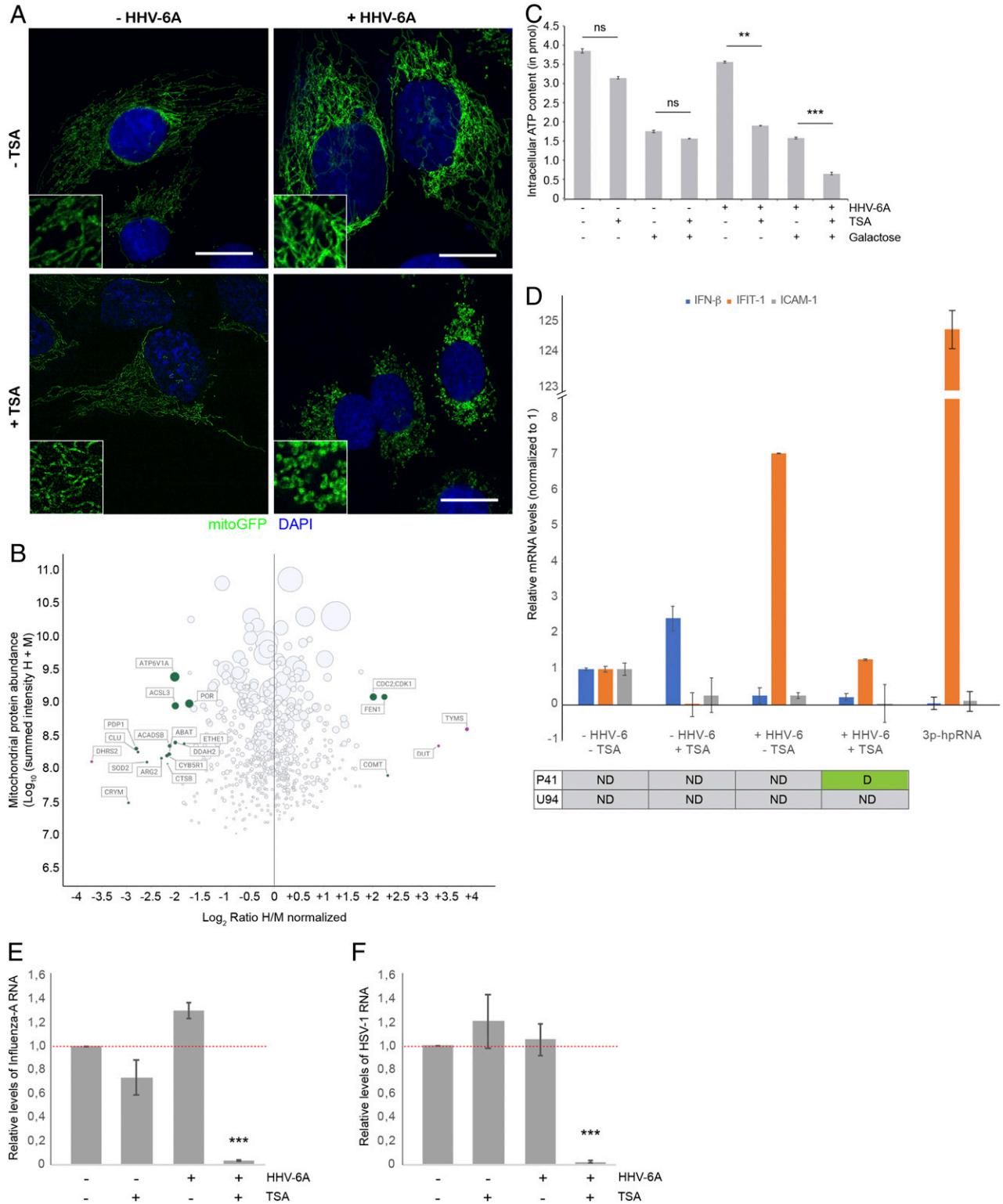


**FIGURE 1. HHV-6A reactivation induces major changes in host cell mitochondrial physiology.**

(A) HHV-6A reactivation alters mitochondrial architecture. U2-OS cells expressing soluble GFP (mitoGFP) within mitochondrial lumen and carrying latent HHV-6A were treated with TSA for 48 h. Control cells without latent virus and without TSA were processed in parallel. Cells were fixed and mitochondrial architecture was quantified using SIM. Magnified images of mitochondria are shown within insets. Scale bar, 10 μm. (B) Normalized values of fold change in mitochondrial protein expression during HHV-6A reactivation in U2-OS cells from two independent pSILAC experiments. Circles indicate identified mitochondrial proteins; circle size correlates with the number of peptides used for quantification. (Continued)

HHV-6A in these cells using the histone deacetylase inhibitor TSA and studied ATP content upon virus reactivation. To measure mitochondrial ATP generation alone in the absence of glycolytic ATP machinery, we replaced glucose-containing media with a galactose-containing media in parallel sets of experiments. Galactose cannot be efficiently metabolized to pyruvate anaerobically and forces cells to shift to mitochondrial oxidative phosphorylation for energy metabolism and survival (33). Our results showed a decrease in both cytoplasmic as well as mitochondrial ATP upon HHV-6A reactivation (Fig. 1C). The possibility of loss of ATP because of productive viral life cycle was eliminated, as HHV-6A has a nonproductive life cycle in these cells.

HHV-6A reactivation within U2-OS cells would lead to an innate immune response. However, like many other viruses (reviewed in Ref. 34), HHV-6A might also have evolved a mechanism to induce mitochondrial fission. Mitochondrial fission reduces the cell's ability to mount innate immune response (reviewed in Ref. 24). To check this, we evaluated IFN response in U2-OS cells upon virus reactivation using qRT-PCR. mRNA levels of IFN- $\beta$ , IFN-responsive and viral RNA-binding gene IFIT-1, and TNF- $\alpha$  response gene ICAM-1 were quantified. U2-OS cells transfected with 3p-hpRNA were used as a positive control. Our results showed decreased innate immune response in U2-OS cells upon virus reactivation (Fig. 1D), having lower IFN- $\beta$  and TNF- $\alpha$  mRNA levels. Interestingly, we observed comparatively higher IFIT-1 mRNA levels in the presence of latent HHV-6A before stimulation with TSA. Increased ISG response, particularly retinoic acid-inducible gene I (RIG-I)-stimulated genes, such as IFIT-1, in latent virus-containing cells, strengthens our argument that mitochondrial fragmentation might be an adaptation by the virus to avoid innate immune response at the time of viral reactivation when viral IE RNAs are freely available in host cell cytoplasm. Fragmented mitochondria are inefficient in providing strong innate immune response, as they prevent interaction between mitochondrial antiviral signaling protein (MAVS) and stimulator of IFN genes (STING) at mitochondria-associated membranes (24). The possibilities of productive viral life cycle in U2-OS cells was eliminated by quantifying P41 and U94 mRNAs (Fig. 1D) in the same mRNA preparations. HHV-6 P41, an IE viral

protein that has been implicated during the early phases of viral replication, was detected upon TSA treatment (Fig. 1D), supporting our previous data (15). At the same time, viral protein U94 was not detected after 48 h of TSA treatment (Fig. 1D), which demonstrates that virus reactivation was incomplete. We have also previously shown lack of U94 transcription upon HHV-6A reactivation in U2-OS cells by transcriptomics studies (15). Thus, our results show that partial reactivation of HHV-6A is enough to induce mitochondrial fragmentation that leads to lower ATP content in the cells accompanied by lower innate immune response.

### ***Proinflammatory mitochondrial architecture can be transmitted through secreted factors from HHV-6-reactivated cells***

Such an altered respiratory state of the cell, accompanied by a decrease in mitochondrial oxidative phosphorylation and fragmented mitochondrial architecture (M1 mitochondria) has been suggested to increase proinflammatory cell danger response (CDR) (35, 36) and serve a critical role in cellular defense against microbial pathogens. To test this hypothesis, we developed an assay system using human A549 lung carcinoma cells as a readout. A549 cells were pretreated with culture supernatant from U2-OS cells with and without integrated HHV-6A for 48 h. Cells were then washed thoroughly and challenged with an RNA (influenza-A) or DNA virus (HSV-1) infection at an MOI of 1. Twenty-four hours postinfection, cells were collected, and the viral infection was quantified using qRT-PCR against one of the early viral RNAs. Viral M1 RNA was used as an indicator of influenza virus infection, and ICPO RNA was used as an indicator of HSV-1 infection. Our results showed that culture supernatants only from cells containing ciHHV-6 DNA that was transactivated could provide protection against both HSV-1 and influenza-A (Fig. 1E, 1F). Indirect effects of viral reactivation drugs were eliminated by using cells that did not carry latent viral genome but were still treated with the reactivating drug (TSA). These results showed that cells containing latent HHV-6A DNA that had been transactivated by TSA secreted a potent activity that could be adoptively transferred and induce mitochondrial fragmentation and a proinflammatory CDR

Mitochondrial proteins having high and moderate but significant changes in expression are indicated in pink and green color, respectively. Gray color indicates proteins having insignificant changes in expression. (C) Intracellular ATP content is decreased upon HHV-6A reactivation. Total intracellular ATP content was measured after 48 h of viral reactivation as shown in (A). In a parallel experiment, cell culture media were replaced with galactose-containing media 8 h prior to ATP measurement. (D) IFN and TNF- $\alpha$  response in U2-OS cells carrying reactivated HHV-6A. IFN and TNF- $\alpha$  response was studied in an experimental setup as shown in (A) by quantifying mRNA levels of IFN- $\beta$ , IFIT-1, and ICAM-1. HHV-6 genes P41 and U94 were also amplified in the same samples to test viral reactivation in the cells. RNA derived from 3p-hpRNA-transfected U2-OS cells were used as a positive control for IFN response. Data represent mean values of two independent biological replicates. (E) Adoptive transfer of culture supernatant from HHV-6A-reactivated cells to healthy cells inhibits influenza-A infection. influenza-A infection was compared by measuring viral RNA in A549 cells treated with culture supernatant from U2-OS cells with or without latent HHV-6A. (F) Adoptive transfer of culture supernatant from HHV-6A-reactivated cells to healthy cells inhibits HSV-1 infection. HSV-1 infection was compared by measuring viral RNA in A549 cells treated with culture supernatant from U2-OS cells with or without latent HHV-6A. (D and E) Data represent mean values of three independent experiments. Relative quantity of 1 is marked as a baseline (dotted line). \*\* $p < 0.01$ , \*\*\* $p < 0.001$ . D, detected; H, heavy isotope; M, medium isotope; ND, not detected.

in naive responder cells, conferring strong protection from both DNA and RNA virus infections. However, it is not necessary that both the mitochondrial fragmentation and antiviral protection phenotypes are dependent on each other and are caused by the same factor.

Based upon the above results, we asked the following question: can cell-free culture supernatant from HHV-6A-reactivated cells cause similar changes in mitochondrial architecture of nearby cells? Hence, we collected cell-free culture supernatant from U2-OS cells after 2 d of viral reactivation and incubated them with fresh U2-OS cells without carrying any virus but expressing a soluble mitochondrial GFP (mitoGFP) (Fig. 2A). Solvent control-treated cell-free culture supernatant as well as cell-free culture supernatant from non-virus-containing cells served as control. Upon analyzing mitochondrial architecture, we detected significant changes in mitochondrial morphology upon incubation of healthy cells with cell-free culture supernatant obtained from HHV-6A-reactivated cells (Fig. 2B, 2C). Increased mitochondrial fragmentation, thus leading to decreased average mitochondrial surface area (Fig. 2C), was observed in those cells that were treated with culture supernatants from HHV-6A-reactivated cells in comparison with controls. This effect of viral reactivation on mitochondrial morphology of nearby cells provided an interesting scenario that could be used to study ME/CFS pathophysiology. A transferrable hypometabolic phenotype in responder cells was further supported by observations of decreased intracellular ATP content (Fig. 2D). A potential role of increased immune response in responder cells serving as an antiviral factor was eliminated by quantifying IFN response in these cells (Fig. 2E, Supplemental Fig. 2A). A very mild (up to 2–3-fold) increase in IFN- $\beta$  and TNF- $\alpha$  response was detected in the U2-OS cells carrying latent virus independent of the drug TSA (Fig. 2E). However, a potential viral RNA-induced immune response was eliminated in both U2-OS (Fig. 2E) and A549 cells (Supplemental Fig. 2A) because of a lack of induced IFIT-1 mRNA. These results suggested that an unknown and IFN-independent transferrable factor from HHV-6A-reactivated cells can induce a hypometabolic, fragmented mitochondrial phenotype in responder cells.

### ***HHV-6 and HHV-7 as a potential causative factor for ME/CFS***

As our *in vitro* HHV-6A reactivation studies pointed toward potential similarities between viral reactivation and ME/CFS pathophysiology, we looked into possibilities of viral cause behind ME/CFS in 25 ME/CFS patients ( $n = 25$ ) and 10 control samples ( $n = 10$ ) using DNA qPCR. We argued that high viral load should be detected in the blood of ME/CFS patients to associate viral infection to the disease. Patients diagnosed with ME/CFS based on Canadian Consensus Criteria were randomly selected and ranged between the age of 21–59 y. Control samples were obtained from healthy non-ME/CFS patients as well as persons with other clinical conditions. DNA was extracted from total blood, isolated PBMCs, serum, and hair follicles of all the patients. Hair follicles were tested for viral DNA to look for potential *ici*HHV-6 cases, which show high viral load (one to two copies per cell). Serum was

tested for extracellular viral DNA that could result from viremia, suggesting potential viral activation/infection.

qPCR studies detected no viral DNA in any of the 25 ME/CFS hair follicle samples (Supplemental Table I). However, two of the controls had  $\sim 1$  copy of either HHV-6A or HHV-6B in hair follicles, suggesting potential *ici*HHV-6A and *ici*HHV-6B individuals, respectively. Similar amounts of viral DNA were detected in blood, PBMCs, and serum samples of these two control individuals, which confirmed latent viral integration. The absence of any viral mRNA in these two cases also reconfirmed a latent viral state in these two individuals. Serum samples from these two individuals were used as controls in all subsequent experiments. Three ME/CFS patients were positive for HHV-6 in total blood-derived DNA samples (Supplemental Table I) as well as in PBMC-derived DNA. Another ME/CFS patient was also diagnosed as HHV-6-positive in PBMC-derived DNA but not in total blood-derived DNA, so only 16% (4 of 25) of CFS patients carried HHV-6 DNA in the blood. A very low-average viral DNA amount in the blood could be due to latent virus or potential viral activation in a very few cells that could result in dilution of viral DNA and RNA in total blood sample. We have recently identified HHV-6-encoded sncRNA-U14 as a potent marker for viral reactivation (15). Expecting that viral RNA numbers under reactivation/infection conditions can be higher than viral DNA numbers and that they should be easier to detect, we carried out FISH studies using concentrated PBMCs or blood clot sections from a fraction of these ME/CFS cases ( $n = 20$ ) (Fig. 3). FISH analysis increased HHV-6-positive cases to 40% ( $n = 8$  out of 20) (Supplemental Table I). FISH image analysis confirmed our hypothesis that only a small fraction of the blood cells carried HHV-6 sncRNA-U14. None of the control cases, including the two *ici*HHV-6 cases, showed positive staining for sncRNA-U14. Thirty-six percent of our ME/CFS patients tested positive for HHV-7 DNA, with an average viral DNA of 1,835–26,056 copies per million cells. We did not characterize latent or active HHV-7 infection in our samples. In conclusion, we detected very low copies of viral genome in ME/CFS patients, which was not enough to point to any direct role of active viral infection in the disease.

### ***Serum from ME/CFS patients but not controls induced changes in mitochondrial architecture of healthy cells***

Low copies of virus DNA and RNA in blood of ME/CFS patients created a confusing scenario in which it is hard to understand the causal role of these viruses in disease progression. A plausible explanation can be localized viral infection/activation in distant parts of the body, thereby releasing a few infected cells carrying activated virus or releasing some of the activation-mediated cellular factors into the blood stream. Interestingly, previous work (28) has showed that serum from ME/CFS patients with severe disease increases rates of mitochondrial oxidative metabolism and respiration in healthy muscle cells under conditions of energetic strain. We thus asked if serum from ME/CFS patients can alter mitochondrial morphology in healthy cells in a similar way, as observed with HHV-6 infection. We thus grew U2-OS cells having soluble mitoGFP but no HHV-6 in the presence of serum from

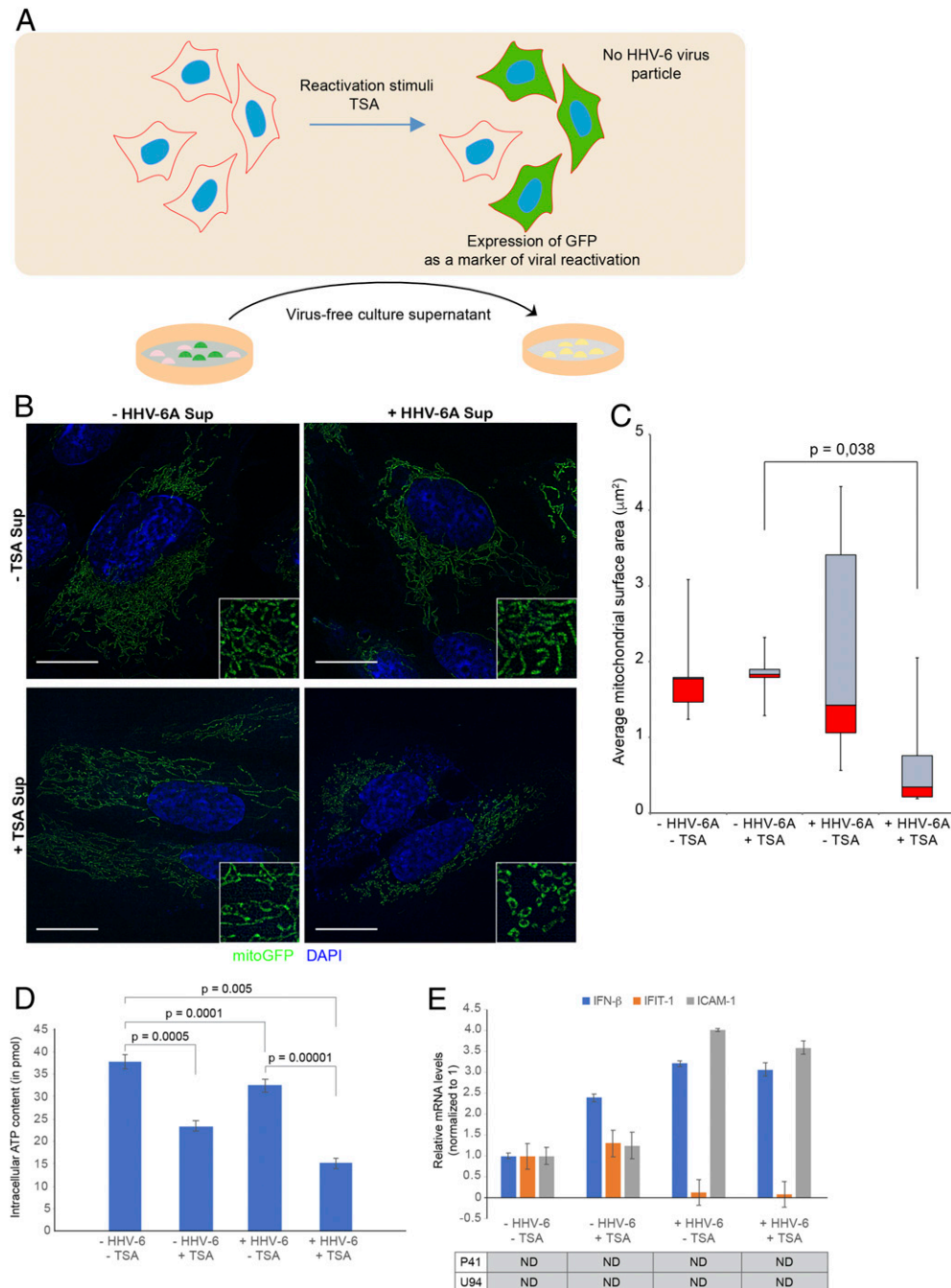


**FIGURE 2. Adoptive transfer of culture supernatant from HHV-6A–reactivated cells induces alterations in mitochondrial dynamics.**

(A) Schematics of experimental setup for adoptive transfer assays using culture supernatants from U2-OS cells having reactivated HHV-6A. (B) Mitochondrial morphology was studied in U2-OS cells using SIM. Virus reactivation was induced in cells carrying latent HHV-6A using TSA, and then the culture supernatant from these cells was used to grow fresh U2-OS cells without having HHV-6A but carrying soluble GFP within the mitochondria. Culture supernatants from cells not carrying any latent HHV-6A were used as control for similar adoptive transfer experiments. SIM images were processed using Fiji. Magnified images of mitochondria are shown within insets. Scale bar, 10  $\mu\text{m}$ . (C) Adoptive transfer–mediated changes in mitochondrial morphology in U2-OS cells in the absence of any virus and as observed in (B) were quantified using SIM. Average mitochondrial surface area was measured from the SIM images. (D) Intracellular ATP content is decreased upon adoptive transfer of culture supernatants from HHV-6A–reactivated cells. Total intracellular ATP content was measured in U2-OS cells without having latent HHV-6A, as shown in (B), after 24 h of supernatant treatment. (E) IFN and TNF- $\alpha$  response in U2-OS cells upon adoptive transfer of culture supernatants from reactivated HHV-6A cells. IFN and TNF- $\alpha$  response was studied in an experimental setup as shown in (B) by quantifying mRNA levels of IFN- $\beta$ , IFIT-1, and ICAM-1. HHV-6 genes P41 and U94 were also amplified in the same samples to test presence of virus in the cells. Data represent mean values of two independent biological replicates.

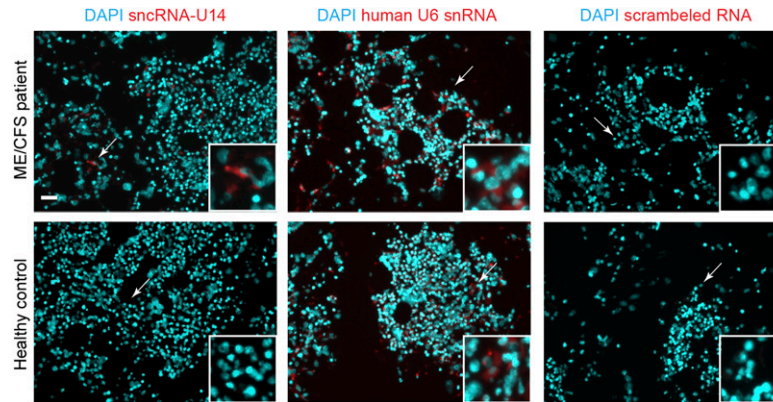


**FIGURE 3. FISH analysis of blood clot sections for presence of HHV-6 sncRNA-U14 in CFS patients and HC.**

Representative images showing FISH analysis for HHV-6 sncRNA-U14, human U6 snRNA (positive control), and a scrambled RNA (negative control). A positive ME/CFS patient (Upper panel) and a negative healthy donor (lower panel) sample-tested for sncRNA-U14 expression is shown. Scale bar, 10  $\mu$ M.

ME/CFS patients as well as control cases (Fig. 4A). Mitochondrial dynamics was analyzed using SIM (Fig. 4B) as well as confocal imaging. Our results showed increased mitochondrial fragmentation as quantified by average mitochondrial surface area in healthy cultured cells upon incubation with serum from ME/CFS patients but not with healthy donor serum (Fig. 4C). Direct quantification of mitochondrial surface area in PBMCs of ME/CFS patients was not very helpful, as PBMCs are smaller in size and have a rounded shape that constrains mitochondrial elongation and hinders quantification of mitochondrial size. Our results suggest that alterations in mitochondrial architecture to acquire a more M1-proinflammatory form of mitochondria is an important characteristic feature in ME/CFS patients and does not require direct viral infection in every cell.

#### **Serum-transferrable innate immunity in ME/CFS patients**

As increased CDR was a transferrable feature of HHV-6A reactivation in vitro, we tested whether a similar proinflammatory activity could be measured in the blood of ME/CFS patients. As an assay system, we grew A549 cells in the presence of serum from 10 ME/CFS patients and five controls. After 2 d of serum exposure, cells were washed and exposed to influenza-A or HSV-1 at a low MOI of 1. Quantification of viral infection revealed up to 99% decrease in viral infection of both HSV-1 and influenza upon serum treatment of ME/CFS patients (Fig. 5A, 5B). Only one out of 10 ME/CFS patients did not have any negative effect of influenza-A infection. In fact, we observed 2.5-fold increase in influenza infection in the presence of serum from this patient. Four of the five control serums did not have any negative effect on influenza-A infection. Only one of the control serums decreased influenza infection up to 50%. However, this decrease was not comparable to the extent of protection that we observed in presence of ME/CFS serum samples. In the case of HSV-1 infection, none of the control serum samples provided antiviral protection (Fig. 5A, 5B). Contingency table analysis showed strong significance and excellent performance characteristics for the diagnostic utility of this assay

system. The positive predictive value for the influenza-A inhibition assay in identifying serum from patients with ME/CFS was 0.9 (95% CI = 0.6–0.99;  $p = 0.017$ ) (Supplemental Table II). The positive predictive value for the HSV-1 inhibition assay was 1.0 (95% CI = 0.72–1.0;  $p = 0.0003$ ) (Supplemental Table II). To test the possibility of a hypometabolic state in the responder A549 cells, we measured intracellular ATP levels in A549 cells upon incubation with ME/CFS patient serum or HC serum. We observed a lower intracellular ATP level in these cells (Fig. 5C). However, because of the smaller sample size we could not observe a statistically significant difference in ATP content. A graphical summary of the assay system is shown in Fig. 6.

#### **Ruling out TNF- $\alpha$ and IFN response**

One of the most prominent candidate molecules that can provide strong antiviral defense is IFN. Hence, we tested IFN response in A549 cells upon treatment with ME/CFS or HC serum. We observed a strong decrease in mRNA levels of IFN- $\beta$ , IFIT-1, and ICAM-1 within the A549 cells in presence of ME/CFS serum in comparison with HC serum (Fig. 5D–F). Then we asked whether the secretory IFN response in isolated PBMCs is higher in ME/CFS patients. For this we used a different cohort of 22 CFS patients and 22 HC. Upon challenge with LPS, we found lower levels of secreted TNF- $\alpha$  ( $p < 0.01$ ) and IFN- $\gamma$  ( $p < 0.05$ ) from CFS patient PBMCs compared with HC (Supplemental Fig. 2B). No significant differences were seen for IL-1 and IL-5. These results ruled out a potential role of IFN response in the mitochondrial fragmentation and antiviral response in ME/CFS patients.

## **DISCUSSION**

HHV-6 infection and reactivation alter host cell transcriptome, including the miRNAome (15, 37, 38). miRNAs regulate intracellular mechanisms, in which they perform the job of fine-tuning of the functions required to fulfill the metabolic demands of

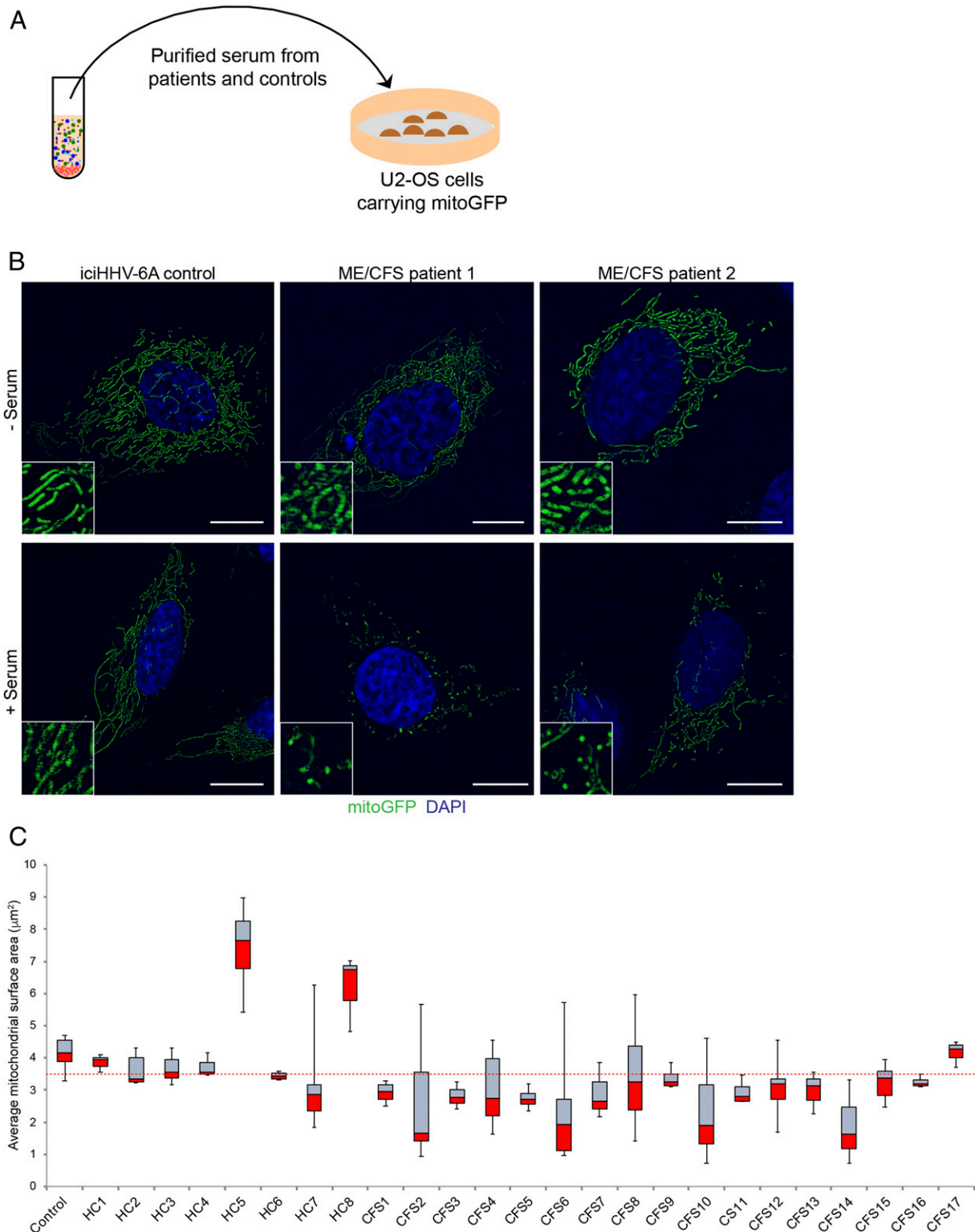


**FIGURE 4. Adoptive transfer of serum from CFS patients and HC induces alterations in mitochondrial dynamics.**

(A) Schematic of experimental setup for adoptive serum treatment assays. (B) Mitochondrial morphology was studied in U2-OS cells carrying soluble mitoGFP. SIM images were processed using Fiji. Representative images from two CFS patients' serum and a control non-CFS person with iciHHV-6 (latent) serum-treated cells are shown. Magnified images of mitochondria are shown within insets. Scale bar, 10  $\mu\text{m}$ . (C) Average mitochondrial surface area was measured from U2-OS cells after serum treatment using SIM imaging. Control represents cells without any serum treatment. Relative average surface area of mitochondria in untreated cells is marked as a baseline (dotted line).

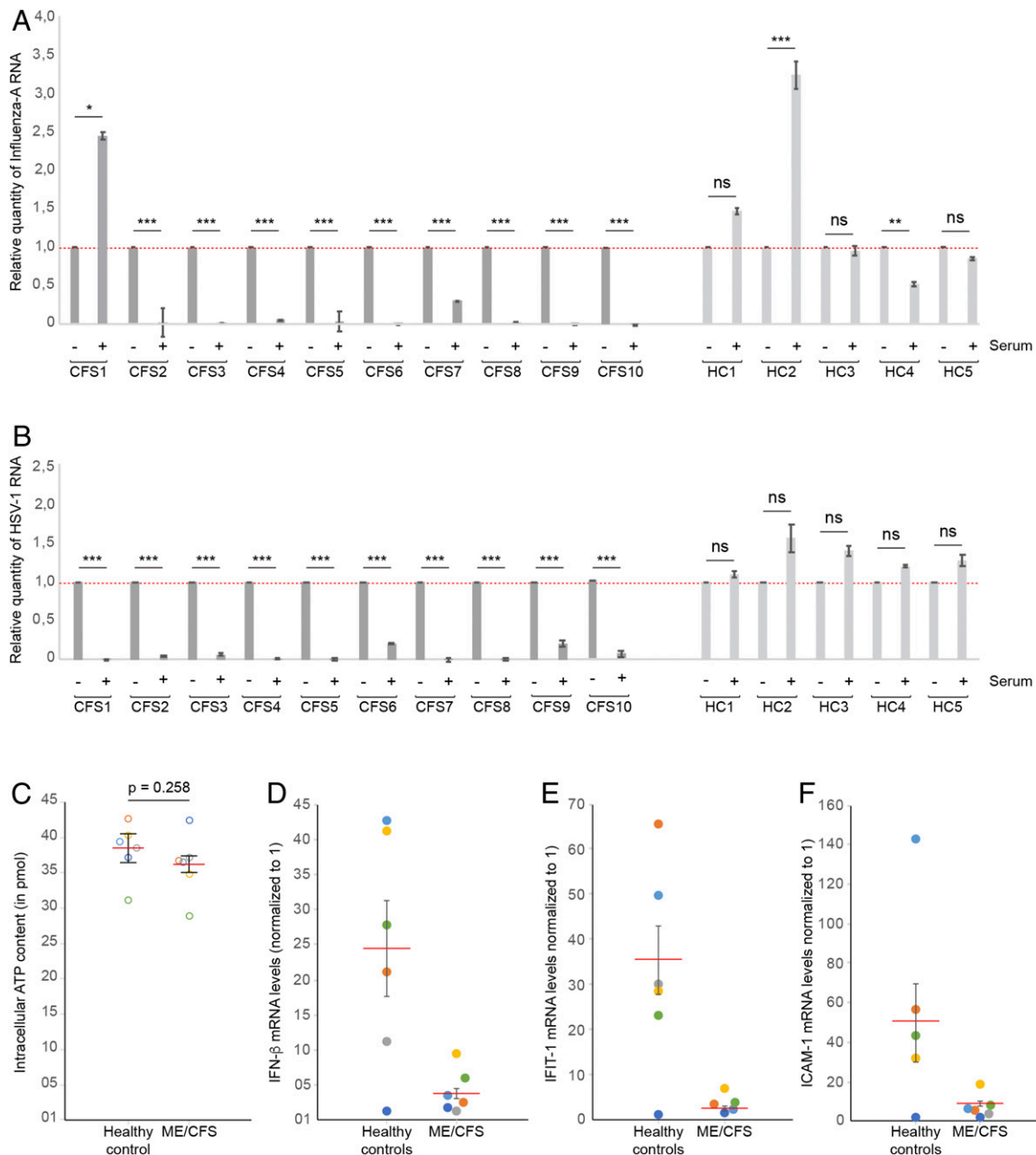


**FIGURE 5. Adoptive transfer of serum from CFS patients provides protection against both RNA virus (influenza-A) and DNA virus (HSV-1).**

(A) Influenza-A infection was compared by measuring viral RNA in A549 cells treated with serum samples from ME/CFS patients or controls. (B) HSV-1 infection was compared by measuring viral RNA in A549 cells treated with serum samples from ME/CFS patients or controls. (A and B) Data represent mean values of three independent experiments. Relative quantity of 1 is marked as a baseline (dotted line).  $p < 0.05$ ,  $p^{**} < 0.01$ ,  $p^{***} < 0.001$ . (C) Intracellular ATP content is marginally decreased in presence of ME/CFS patient serum. Total intracellular ATP content was measured in A549 cells after 48 h of treatment of cells with either CFS patient serum or HC serum. Data represent mean values of two biological replicates. (D) IFN- $\beta$  mRNA levels in A549 cells are decreased upon adoptive transfer of serum from CFS patients or HC. IFN response was studied in an experimental setup as shown in (A) and (B) by quantifying mRNA levels of IFN- $\beta$ . Data represent mean values of two independent biological replicates. (E) IFN-responsive gene IFIT-1 mRNA was studied in the same experimental setup as above. (F) TNF- $\alpha$  responsive gene ICAM-1 mRNA was studied in the same experimental setup as above.

an organ or cell type. Our previous deep sequencing approach (15) revealed major changes in the expression of a large panel of human miRNAs upon HHV-6A reactivation that hints to a broad range of

effects on mitochondria and associated metabolic functions upon viral activation. In this study, we studied quantitative changes in cellular as well as mitochondrial proteomics upon HHV-6A

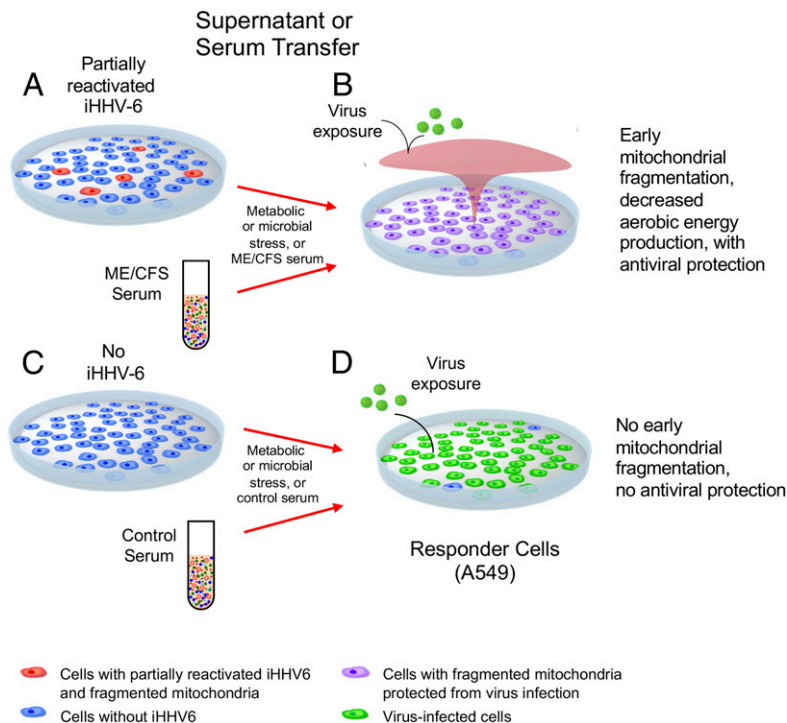


**FIGURE 6. Graphical Summary.**

(A) Mitochondria rapidly fragmented in cells containing integrated HHV-6 (iHHV-6) after partial virus reactivation in response to genetic and/or environmental stress. Mitochondrial fragmentation was associated with a decrease in cellular ATP production and a potent antiviral activity that was secreted into the supernatant. Genetic and environmental stressors were modeled by treatment with the histone deacetylase inhibitor TSA with or without substitution of the nonfermentable carbon source galactose for glucose in the medium. Partial iHHV-6 reactivation was characterized by the production of noncoding RNA but did not result in viral protein synthesis or replication. Red colored cells represent partial iHHV-6 reactivation. (B) When the supernatant of stressed iHHV-6 cells was transferred to responder cells, a potent antiviral activity was found. This secreted activity was distinct from IFN and TNF- $\alpha$  and was indistinguishable from the activity found in serum from patients with ME/CFS. The mitochondrial fragmentation, metabolic, and antiviral properties of this iHHV-6 cell–secreted and ME/CFS serum activity appeared to transfer together and could not be separated in this study. The antiviral activity had broad specificity. This activity prevented infection with either the RNA virus influenza-A or the DNA virus HSV-1. Purple cells represent cells with fragmented mitochondria, which, were resistant to virus infection. (C) Cells that lacked iHHV-6 could not be induced to secrete the antiviral and mitochondrial fragmentation activities found in (A). (D) When responder cells were exposed to serum from HC subjects or to supernatant from stressed cells that lacked iHHV-6, no antiviral or mitochondrial fragmentation activity was observed. Green colored cells represent virus-infected cells.

reactivation and found several significant alterations with close similarity to ME/CFS pathophysiology. PDP1 was downregulated in response to HHV-6A reactivation. PDP1 helps in reverting the negative effects of pyruvate dehydrogenase kinases on pyruvate dehydrogenase. A decrease in PDP1 suggests a potential decrease in functions of pyruvate dehydrogenase, which is also reported in ME/CFS patients (28). We also found a decrease in the SOD2 level that can lead to high amount of ROS within the cell. We have previously shown that HHV-6 infection induces ROS in host cells and alters expression of glutathione reductase (29). These observations strongly support a pathological link between HHV-6 reactivation and ME/CFS.

Hypometabolic state of blood cells is a characteristic feature of ME/CFS (39). Although we did not perform metabolic studies, our study on mitochondrial architecture in presence of CFS patient serum but not controls has revealed a transferrable activity in ME/CFS serum that fragments mitochondria and stimulates a

coordinated antiviral state in naive responder cells assayed in vitro. This assay was highly sensitive (0.9–1.00; 95% CI = 0.6–1.0) and specific (0.8–1.0; 95% CI = 0.38–1.0) in identifying serum from patients with ME/CFS. In our studies, both viral reactivation as well as CFS patient serum treatment induced a typical M1 state of mitochondria (35, 36) in host cells, which was also accompanied by a strong proinflammatory state of the cell that protected the host cells against both incoming DNA and RNA viruses, consistent with oxidative shielding (27). There are many possible ways that a nearby healthy cell can sense potential infectious risk in the environment. Increased IFN response from the virus-transactivated cells can result in secreted IFN that can be sensed by the nearby cells, leading to a hypometabolic state (40). Several type I and type II IFNs, as well as IFN response genes, are reported to be high in the serum of ME/CFS patients (41, 42). However, we did not observe any increase in IFN- $\gamma$  in PBMCs of a small group of ME/CFS patients (Supplemental Fig. 2B). In addition, we observed significant

decrease in ISG expression upon treatment with ME/CFS serum. Hence, the strong antiviral phenotype in our assay system seems to be IFN-independent. Fragmented mitochondria can release broken mitochondrial DNA into the cytoplasm (43) and to the extracellular space that can induce TLR-mediated cytokine production in nearby cells (44). Newly synthesized, 8-hydroxyguanosine-containing mitochondrial DNA (ox-mtDNA) can directly activate assembly of the NLRP3 inflammasome (45). Interestingly excess of certain cytokines can also change mitochondrial metabolism (46) to prevent further pathogen growth. Certain complex disorders, such as amyotrophic lateral sclerosis, are associated with a hypometabolic state that is characterized by lower mitochondrial size and number (47–49).

Autoimmunity is common in ME/CFS (50). Several autoantibodies are capable of inducing a proinflammatory state in target cells (51). Interestingly, HHV-6 is linked to several autoimmune diseases, including multiple sclerosis and Hashimoto thyroiditis (52). Autoantibodies against  $\beta_2$  adrenergic receptors ( $\beta_2R$ ) were found to be upregulated in a subset of patients with ME/CFS (53). Such Abs belong to a network of natural Abs against adrenergic, acetylcholine (cholinergic), and other GPCR receptors that were shown to be dysfunctional in various autoimmune diseases (54). Autonomic dysregulation is a hallmark of ME/CFS. There is evidence that the  $\beta_2R$ -mediated regulation of cytokines by terbutaline is impaired in whole blood immune cells of CFS patients (55). A recent paper showed that influenza replication is inhibited by  $\alpha_2$  adrenergic stimulation via cAMP inhibition (56). In contrast  $\beta_2R$  stimulation is known to stimulate cAMP. Thus, a disbalance of adrenergic stimulation favoring cAMP downregulation might also be an explanation for our findings. However, similarities between adoptive transfer of HHV-6A reactivation culture supernatant and ME/CFS serum suggests a potential metabolic role in addition to other possibilities.

Lack of a strong HHV-6 and HHV-7 infection in ME/CFS patients in our study and several others has historically cast doubt on the involvement of these viruses in ME/CFS. However, in this study, we show that incomplete HHV-6 reactivation, even in a small fraction of latently infected cells, causes reactivated cells to secrete an activity that can be transferred in serum and produces mitochondrial fragmentation and coordinates a powerful antiviral program in responding cells. Our studies showed that only IE events, such as the transcription of several small noncoding viral RNAs, were needed to trigger the production and secretion of the mitochondrial fragmentation factor and transferrable antiviral state. No HHV-6 proteins are made during the incomplete reactivation events described in this paper. Specifically, no major change in HHV-6 replication was observed. This explains the failure of anti-herpesvirus drugs in a subset of patients because the HHV-6 polymerase is not expressed during an incomplete virus reactivation, and drugs that target the viral DNA polymerase would have no viral target.

The virus reactivation experiments described in this study show that an antiviral state is produced both in cells with unreactivated and reactivated HHV-6. This seems to be against the viral growth and hence fails to explain the short-term benefits of

viral reactivation from the pathogen point of view, unless passive transmission of viral genome to daughter cells after mitosis plays a major role in HHV-6 genome propagation. Decreased IFN response in virus-reactivated cells might provide an advantage for survival of IE RNAs in the host cell cytoplasm. However, in this study, we have tested only the nonproductive transactivation state of the virus. Productive viral infection, with virion production and release, might bring in additional viral factor(s) that damage cellular ability to undergo a hypometabolic state to provide successful virus growth. Additionally, mitochondrial fragmentation often allows virus to acquire persistent or latent state under a hypometabolic state (57).

In this study, we found that none of 25 patients with ME/CFS had peripheral blood evidence of a fully reactivated HHV-6 or HHV-7 infection, and only 8 of 20 (40%; 95% CI = 0.19–0.64) had evidence of partial reactivation measured by FISH analysis of HHV-6 small noncoding RNA U14 in whole blood. However, using an *in vitro* reporter cell assay, we showed that serum from ME/CFS patients contained an activity that produced mitochondrial fragmentation, decreased mitochondrial ATP production, and induced a powerful antiviral state. In 2016, metabolomic analysis of patients with ME/CFS revealed a chemical signature that was similar to the evolutionarily conserved, hypometabolic state known as *dauer* (39). This *dauer*-like state was preserved by blocks to healing produced by abnormal persistence of the CDR (36). The CDR has been shown to be directly involved in both healing and the biology of aging (35). In this earlier work, it was hypothesized that the metabolic features of the CDR in ME/CFS patients could protect against certain kinds of infection, but no direct testing for antiviral activity was performed (39). Our current data show that only a small fraction of cells need to be latently infected with HHV-6 to trigger a secretory phenotype that is strongly protective against some of the RNA and DNA virus infection in neighboring and distant cells lacking HHV-6 DNA. The main conclusions of this study are illustrated in the graphical summary (Fig. 6). Larger multicohort studies involving ME/CFS patients from different age groups should be carried out in the future and should include methods for detecting and quantifying both productive and nonproductive (incomplete) viral reactivation events. Furthermore, potential factors affecting mitochondrial dynamics in ME/CFS patients should be systematically evaluated for their ability to induce a powerful antiviral state. Our mitochondrial reporter-based cell system will provide an opportunity to develop a diagnostic test for ME/CFS as well as provide a platform for further identification of potential factors that define ME/CFS pathophysiology.

## DISCLOSURES

The authors have no financial conflicts of interest.

## ACKNOWLEDGMENTS

We thank the patients and families with ME/CFS and HC for helping to make this research possible. We thank Dr. Simone Bakes for providing influenza-A viral preparations for this study. We also thank Dr. Suvagata

Roy Chowdhury for help with SIM. We thank Scott McAvoy at the University of California San Diego Digital Media Lab for help in creating the graphical summary in Fig. 6. Finally, we thank Dr. Archana Prusty for constant support and advice during the biochemical studies.

## REFERENCES

- Morissette, G., and L. Flamand. 2010. Herpesviruses and chromosomal integration. *J. Virol.* 84: 12100–12109.
- Tanaka-Taya, K., J. Sashihara, H. Kurahashi, K. Amo, H. Miyagawa, K. Kondo, S. Okada, and K. Yamanishi. 2004. Human herpesvirus 6 (HHV-6) is transmitted from parent to child in an integrated form and characterization of cases with chromosomally integrated HHV-6 DNA. *J. Med. Virol.* 73: 465–473.
- Pellett, P. E., D. V. Ablashi, P. F. Ambros, H. Agut, M. T. Caserta, V. Descamps, L. Flamand, A. Gautheret-Dejean, C. B. Hall, R. T. Kamble, et al. 2012. Chromosomally integrated human herpesvirus 6: questions and answers. *Rev. Med. Virol.* 22: 144–155.
- Levy, J. A., F. Ferro, D. Greenspan, and E. T. Lennette. 1990. Frequent isolation of HHV-6 from saliva and high seroprevalence of the virus in the population. *Lancet* 335: 1047–1050.
- Cone, R. W., M. L. Huang, R. Ashley, and L. Corey. 1993. Human herpesvirus 6 DNA in peripheral blood cells and saliva from immunocompetent individuals. *J. Clin. Microbiol.* 31: 1262–1267.
- Prusty, B. K., N. Gulve, S. Rasa, M. Murovska, P. C. Hernandez, and D. V. Ablashi. 2017. Possible chromosomal and germline integration of human herpesvirus 7. *J. Gen. Virol.* 98: 266–274.
- Ablashi, D. V., H. B. Eastman, C. B. Owen, M. M. Roman, J. Friedman, J. B. Zabriskie, D. L. Peterson, G. R. Pearson, and J. E. Whitman. 2000. Frequent HHV-6 reactivation in multiple sclerosis (MS) and chronic fatigue syndrome (CFS) patients. *J. Clin. Virol.* 16: 179–191.
- Chapenko, S., A. Krumina, S. Kozireva, Z. Nora, A. Sultanova, L. Viksna, and M. Murovska. 2006. Activation of human herpesviruses 6 and 7 in patients with chronic fatigue syndrome. *J. Clin. Virol.* 37(Suppl. 1): S47–S51.
- Chapenko, S., A. Krumina, I. Logina, S. Rasa, M. Chistjakovs, A. Sultanova, L. Viksna, and M. Murovska. 2012. Association of active human herpesvirus-6, -7 and parvovirus b19 infection with clinical outcomes in patients with myalgic encephalomyelitis/chronic fatigue syndrome. *Adv. Virol.* 2012: 205085.
- Myhill, S., N. E. Booth, and J. McLaren-Howard. 2009. Chronic fatigue syndrome and mitochondrial dysfunction. *Int. J. Clin. Exp. Med.* 2: 1–16.
- Morris, G., and M. Maes. 2014. Mitochondrial dysfunctions in myalgic encephalomyelitis/chronic fatigue syndrome explained by activated immuno-inflammatory, oxidative and nitrosative stress pathways. *Metab. Brain Dis.* 29: 19–36.
- Witte, M. E., D. J. Mahad, H. Lassmann, and J. van Horssen. 2014. Mitochondrial dysfunction contributes to neurodegeneration in multiple sclerosis. *Trends Mol. Med.* 20: 179–187.
- Mao, P., and P. H. Reddy. 2010. Is multiple sclerosis a mitochondrial disease? *Biochim. Biophys. Acta* 1802: 66–79.
- Esfandyarpour, R., A. Kashi, M. Nemat-Gorgani, J. Wilhelmy, and R. W. Davis. 2019. A nanoelectronics-blood-based diagnostic biomarker for myalgic encephalomyelitis/chronic fatigue syndrome (ME/CFS). *Proc. Natl. Acad. Sci. USA* 116: 10250–10257.
- Prusty, B. K., N. Gulve, S. R. Chowdhury, M. Schuster, S. Stempel, V. Descamps, and T. Rudel. 2018. HHV-6 encoded small non-coding RNAs define an intermediate and early stage in viral reactivation. *NPJ Genom. Med.* 3: 25.
- Chowdhury, S. R., A. Reimer, M. Sharan, V. Kozjak-Pavlovic, A. Eulalio, B. K. Prusty, M. Fraunholz, K. Karunakaran, and T. Rudel. 2017. *Chlamydia* preserves the mitochondrial network necessary for replication via microRNA-dependent inhibition of fission. *J. Cell Biol.* 216: 1071–1089.
- Prusty, B. K., N. Gulve, S. Rasa, M. Murovska, P. C. Hernandez, and D. V. Ablashi. 2017. Possible chromosomal and germline integration of human herpesvirus 7. *J. Gen. Virol.* 98: 266–274.
- Gulve, N., C. Frank, M. Klepsch, and B. K. Prusty. 2017. Chromosomal integration of HHV-6A during non-productive viral infection. *Sci. Rep.* 7: 512.
- Prusty, B. K., N. Gulve, S. Govind, G. R. F. Krueger, J. Feichtinger, L. Larcombe, R. Aspinall, D. V. Ablashi, and C. T. Toro. 2018. Active HHV-6 infection of cerebellar Purkinje cells in mood disorders. *Front. Microbiol.* 9: 1955.
- Prusty, A. B., R. Meduri, B. K. Prusty, J. Vanselow, A. Schlosser, and U. Fischer. 2017. Impaired spliceosomal UsnRNP assembly leads to Sm mRNA down-regulation and Sm protein degradation. *J. Cell Biol.* 216: 2391–2407.
- Cox, J., and M. Mann. 2008. MaxQuant enables high peptide identification rates, individualized p.p.b.-range mass accuracies and proteome-wide protein quantification. *Nat. Biotechnol.* 26: 1367–1372.
- Perez-Riverol, Y., A. Csordas, J. Bai, M. Bernal-Llinares, S. Hewapathirana, D. J. Kundu, A. Inuganti, J. Griss, G. Mayer, M. Eisenacher, et al. 2019. The PRIDE database and related tools and resources in 2019: improving support for quantification data. *Nucleic Acids Res.* 47: D442–D450.
- West, A. P., W. Khoury-Hanold, M. Staron, M. C. Tal, C. M. Pineda, S. M. Lang, M. Bestwick, B. A. Duguay, N. Raimundo, D. A. MacDuff, et al. 2015. Mitochondrial DNA stress primes the antiviral innate immune response. *Nature* 520: 553–557.
- West, A. P., G. S. Shadel, and S. Ghosh. 2011. Mitochondria in innate immune responses. *Nat. Rev. Immunol.* 11: 389–402.
- Gravel, A., I. Dubuc, N. Wallaschek, S. Gilbert-Girard, V. Collin, R. Hall-Sedlak, K. R. Jerome, Y. Mori, J. Carbonneau, G. Boivin, et al. 2017. Cell culture systems to study human herpesvirus 6A/B chromosomal integration. *J. Virol.* 91: e00437.
- Kennedy, G., V. A. Spence, M. McLaren, A. Hill, C. Underwood, and J. J. Belch. 2005. Oxidative stress levels are raised in chronic fatigue syndrome and are associated with clinical symptoms. *Free Radic. Biol. Med.* 39: 584–589.
- Naviaux, R. K. 2012. Oxidative shielding or oxidative stress? *J. Pharmacol. Exp. Ther.* 342: 608–618.
- Fluge, Ø., O. Mella, O. Bruland, K. Risa, S. E. Dyrstad, K. Alme, I. G. Rekeland, D. Sapkota, G. V. Røslund, A. Fosså, et al. 2016. Metabolic profiling indicates impaired pyruvate dehydrogenase function in myalgic encephalopathy/chronic fatigue syndrome. *JCI Insight* 1: e89376.
- Prusty, B. K., L. Böhme, B. Bergmann, C. Siegl, E. Krause, A. Mehlitz, and T. Rudel. 2012. Imbalanced oxidative stress causes chlamydial persistence during non-productive human herpes virus co-infection. *PLoS One* 7: e47427.
- Bach, D., S. Pich, F. X. Soriano, N. Vega, B. Baumgartner, J. Oriola, J. R. Daugaard, J. Lloberas, M. Camps, J. R. Zierath, et al. 2003. Mitofusin-2 determines mitochondrial network architecture and mitochondrial metabolism. A novel regulatory mechanism altered in obesity. *J. Biol. Chem.* 278: 17190–17197.
- Lant, B., and K. B. Storey. 2010. An overview of stress response and hypometabolic strategies in *Caenorhabditis elegans*: conserved and contrasting signals with the mammalian system. *Int. J. Biol. Sci.* 6: 9–50.
- Mishra, P., and D. C. Chan. 2016. Metabolic regulation of mitochondrial dynamics. *J. Cell Biol.* 212: 379–387.
- Rosignol, R., R. Gilkerson, R. Aggeler, K. Yamagata, S. J. Remington, and R. A. Capaldi. 2004. Energy substrate modulates mitochondrial structure and oxidative capacity in cancer cells. *Cancer Res.* 64: 985–993.

34. Kim, S. J., D. G. Ahn, G. H. Syed, and A. Siddiqui. 2018. The essential role of mitochondrial dynamics in antiviral immunity. *Mitochondrion* 41: 21–27.
35. Naviaux, R. K. 2019. Incomplete healing as a cause of aging: the role of mitochondria and the cell danger response. *Biology (Basel)* 8: E27.
36. Naviaux, R. K. 2019. Metabolic features and regulation of the healing cycle—A new model for chronic disease pathogenesis and treatment. *Mitochondrion* 46: 278–297.
37. Rizzo, R., I. Soffritti, M. D'Accolti, D. Bortolotti, D. Di Luca, and E. Caselli. 2017. HHV-6A/6B infection of NK cells modulates the expression of miRNAs and transcription factors potentially associated to impaired NK activity. *Front. Microbiol.* 8: 2143.
38. Caselli, E., M. D'Accolti, I. Soffritti, M. C. Zatelli, R. Rossi, E. Degli Uberti, and D. Di Luca. 2017. HHV-6A in vitro infection of thyrocytes and T cells alters the expression of miRNA associated to autoimmune thyroiditis. *Viol. J.* 14: 3.
39. Naviaux, R. K., J. C. Naviaux, K. Li, A. T. Bright, W. A. Alaynick, L. Wang, A. Baxter, N. Nathan, W. Anderson, and E. Gordon. 2016. Metabolic features of chronic fatigue syndrome. [Published erratum appears in 2017 *Proc. Natl. Acad. Sci. USA* 114: E3749.] *Proc. Natl. Acad. Sci. USA* 113: E5472–E5480.
40. Wu, D., D. E. Sanin, B. Everts, Q. Chen, J. Qiu, M. D. Buck, A. Patterson, A. M. Smith, C. H. Chang, Z. Liu, et al. 2016. Type 1 interferons induce changes in core metabolism that are critical for immune function. *Immunity* 44: 1325–1336.
41. Montoya, J. G., T. H. Holmes, J. N. Anderson, H. T. Maecker, Y. Rosenberg-Hasson, I. J. Valencia, L. Chu, J. W. Younger, C. M. Tato, and M. M. Davis. 2017. Cytokine signature associated with disease severity in chronic fatigue syndrome patients. *Proc. Natl. Acad. Sci. USA* 114: E7150–E7158.
42. Moss, R. B., A. Mercandetti, and A. Vojdani. 1999. TNF-alpha and chronic fatigue syndrome. *J. Clin. Immunol.* 19: 314–316.
43. Bao, D., J. Zhao, X. Zhou, Q. Yang, Y. Chen, J. Zhu, P. Yuan, J. Yang, T. Qin, S. Wan, and J. Xing. 2019. Mitochondrial fission-induced mtDNA stress promotes tumor-associated macrophage infiltration and HCC progression. *Oncogene* 38: 5007–5020.
44. West, A. P., and G. S. Shadel. 2017. Mitochondrial DNA in innate immune responses and inflammatory pathology. *Nat. Rev. Immunol.* 17: 363–375.
45. Zhong, Z., S. Liang, E. Sanchez-Lopez, F. He, S. Shalpour, X. J. Lin, J. Wong, S. Ding, E. Seki, B. Schnabl, et al. 2018. New mitochondrial DNA synthesis enables NLRP3 inflammasome activation. *Nature* 560: 198–203.
46. Maiti, A. K., S. Sharba, N. Navabi, H. Forsman, H. R. Fernandez, and S. K. Lindén. 2015. IL-4 protects the mitochondria against TNF $\alpha$  and IFN $\gamma$  induced insult during clearance of infection with *Citrobacter rodentium* and *Escherichia coli*. *Sci. Rep.* 5: 15434.
47. Hatazawa, J., R. A. Brooks, M. C. Dalakas, L. Mansi, and G. Di Chiro. 1988. Cortical motor-sensory hypometabolism in amyotrophic lateral sclerosis: a PET study. *J. Comput. Assist. Tomogr.* 12: 630–636.
48. Magrané, J., M. A. Sahawneh, S. Przedborski, A. G. Estévez, and G. Manfredi. 2012. Mitochondrial dynamics and bioenergetic dysfunction is associated with synaptic alterations in mutant SOD1 motor neurons. *J. Neurosci.* 32: 229–242.
49. Pickles, S., L. Destroismaisons, S. L. Peyrard, S. Cadot, G. A. Rouleau, R. H. Brown Jr., J. P. Julien, N. Arbour, and C. Vande Velde. 2013. Mitochondrial damage revealed by immunoselection for ALS-linked misfolded SOD1. *Hum. Mol. Genet.* 22: 3947–3959.
50. Sotzny, F., J. Blanco, E. Capelli, J. Castro-Marrero, S. Steiner, M. Murovska, and C. Scheibenbogen, European Network on ME/CFS (EUROMENE). 2018. Myalgic encephalomyelitis/chronic fatigue syndrome - evidence for an autoimmune disease. *Autoimmun. Rev.* 17: 601–609.
51. Elkon, K., and P. Casali. 2008. Nature and functions of autoantibodies. *Nat. Clin. Pract. Rheumatol.* 4: 491–498.
52. Matteoli, B., S. Bernardini, R. Iuliano, S. Parenti, G. Freer, F. Broccolo, A. Baggiani, A. Subissi, F. Arcamone, and L. Ceccherini-Nelli. 2008. In vitro antiviral activity of distamycin A against clinical isolates of herpes simplex virus 1 and 2 from transplanted patients. *Intervirology* 51: 166–172.
53. Loebel, M., P. Grabowski, H. Heidecke, S. Bauer, L. G. Hanitsch, K. Wittke, C. Meisel, P. Reinke, H. D. Volk, Ø. Fluge, et al. 2016. Antibodies to  $\beta$  adrenergic and muscarinic cholinergic receptors in patients with chronic fatigue syndrome. *Brain Behav. Immun.* 52: 32–39.
54. Cabral-Marques, O., A. Marques, L. M. Giil, R. De Vito, J. Rademacher, J. Günther, T. Lange, J. Y. Humrich, S. Klapa, S. Schinke, et al. 2018. GPCR-specific autoantibody signatures are associated with physiological and pathological immune homeostasis. *Nat. Commun.* 9: 5224.
55. Kavelaars, A., W. Kuis, L. Knook, G. Sinnema, and C. J. Heijnen. 2000. Disturbed neuroendocrine-immune interactions in chronic fatigue syndrome. *J. Clin. Endocrinol. Metab.* 85: 692–696.
56. Matsui, K., M. Ozawa, M. Kiso, M. Yamashita, T. Maekawa, M. Kubota, S. Sugano, and Y. Kawaoka. 2018. Stimulation of alpha2-adrenergic receptors impairs influenza virus infection. *Sci. Rep.* 8: 4631.
57. Kim, S. J., G. H. Syed, M. Khan, W. W. Chiu, M. A. Sohail, R. G. Gish, and A. Siddiqui. 2014. Hepatitis C virus triggers mitochondrial fission and attenuates apoptosis to promote viral persistence. *Proc. Natl. Acad. Sci. USA* 111: 6413–6418.

## **SUPPLEMENTARY MATERIALS**

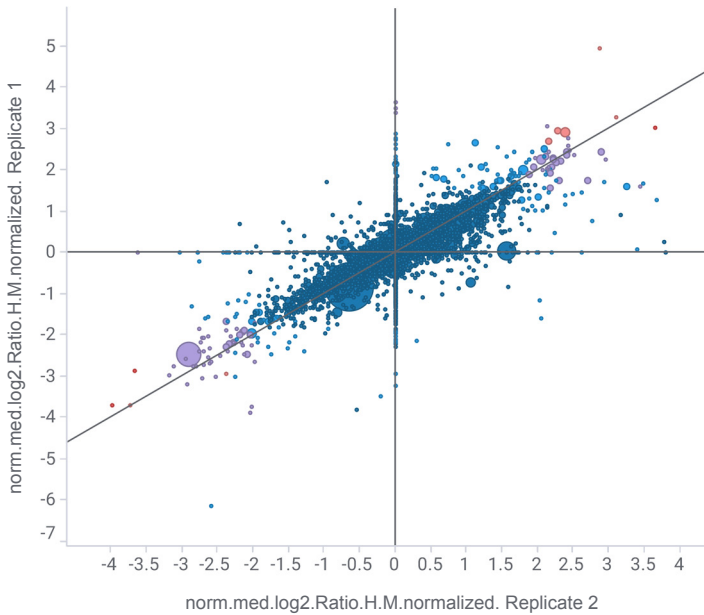
**HHV-6 reactivation, mitochondrial fragmentation, and the coordination of antiviral and metabolic phenotypes in myalgic encephalomyelitis/chronic fatigue syndrome (ME/CFS)**

Schreiner P, et al., 2020

# Figure S1

A

Replicate 1 vs Replicate 2



B

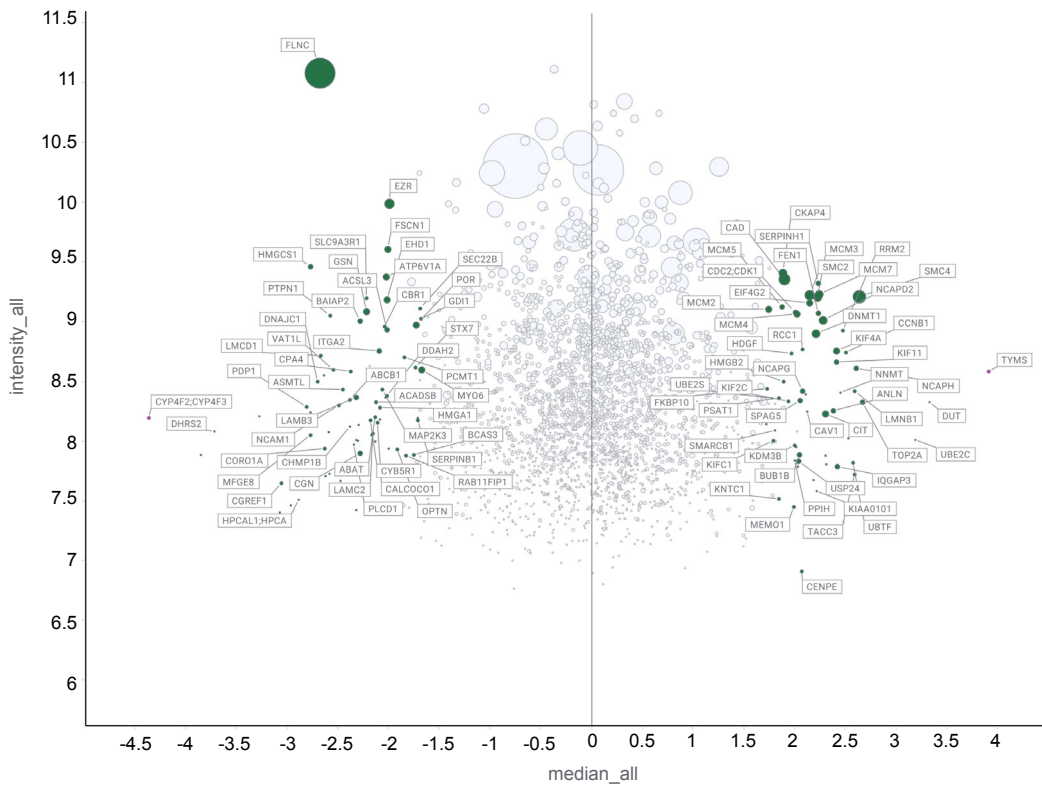


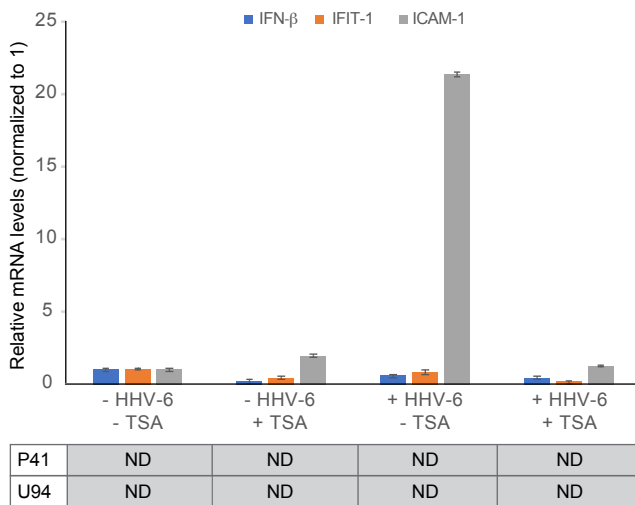
**Figure S1.** HHV-6A reactivation induces major changes in host cell proteomics.

(A) Normalized values of fold change in total protein expression during HHV-6A reactivation from two independent pSILAC experiments. Circles indicate identified cellular proteins. Proteins having significant changes in expression are indicated in different colors. Blue color indicates proteins having insignificant changes in expression whereas purple circles indicate more than 2 fold changed proteins and orange circle indicate the proteins having three fold changes in expression. Proteins from two different (Replicate 1 vs replicate 2) independent experiments are plotted against each other.

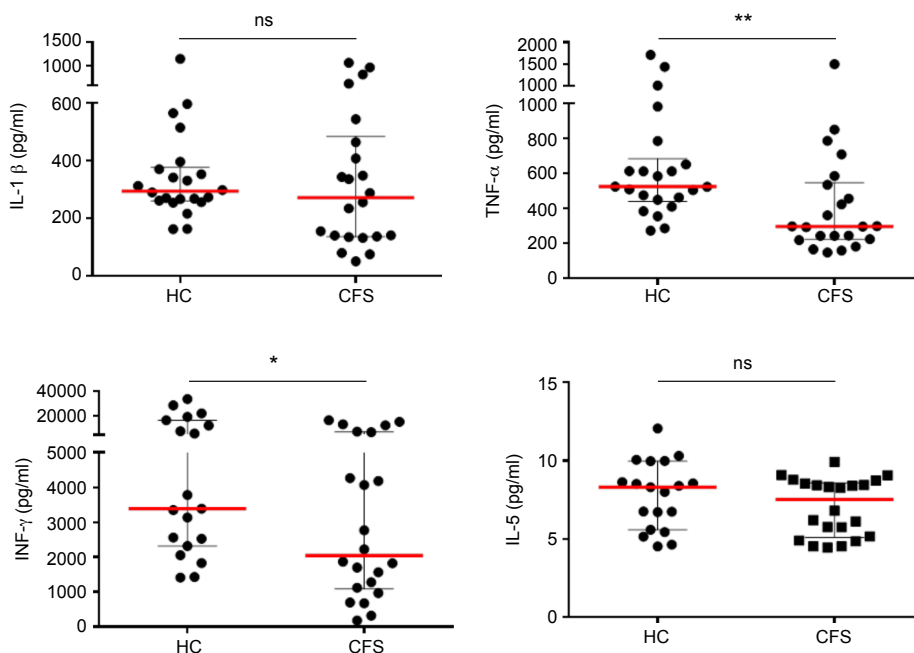
(B) Normalized values of fold change in total cellular protein expression during HHV-6A reactivation from two independent pSILAC experiments. Circles indicate identified various cellular proteins; circle size correlates with the number of peptides used for quantification. Proteins having significant changes in expression are indicated in green and pink color. Gray color indicates proteins having insignificant changes in expression.

Figure S2

A



B



**Figure S2.** Interferon and TNF- $\alpha$  response during adoptive transfer.

(A) Interferon response in A549 cells against adoptive transfer of culture supernatants from U2-OS cells carrying reactivated HHV-6A. A549 cells were treated with sterile filtered culture supernatants from U2-OS cells as shown in Fig.1. 24h post treatment Interferon and TNF- $\alpha$  response was studied by quantifying mRNA levels of IFN- $\beta$ , IFIT-1 (Interferon response gene) and ICAM-1 (TNF- $\alpha$  response gene). HHV-6 genes P41 and U94 were also amplified to test presence of viral infection in the target cells. ND, not detected; TSA, trichostatin-A. Data represents mean values of two independent biological replicates.

(B) Diminished TNF- $\alpha$  and IFN- $\gamma$  levels in CFS patients. The *in vitro* production of TNF- $\alpha$ , IL-1 $\beta$ , IFN- $\gamma$  and IL-5 was comparatively assessed in whole blood stimulated *ex vivo* in 22 patients with CFS and 22 healthy controls (HC).

**Table S1.** Details of qPCR and FISH in patients and healthy controls.

Patient ID	Gender	Age	qPCR using Hair follicle derived DNA		qPCR using total blood derived DNA		qPCR using PBMC derived DNA		Cases included in FISH studies	
			HHV-6 copies/million cells	HHV-7 copies/million cells	HHV-6 copies/million cells	HHV-7 copies/million cells	HHV-6 copies/million cells	HHV-7 copies/million cells	Analysis done	FISH results
MC1	M	59	ND	ND	ND	ND	ND	6000	Yes	Negative
MC2	F	48	ND	ND	ND	ND	ND	15000	Yes	Negative
MC3	F	49	ND	ND	11736	ND	17925	ND	Yes	Positive
MC4	M	25	ND	ND	ND	ND	ND	ND	No	Negative
MC5	F	21	ND	ND	ND	ND	ND	ND	Yes	Negative
MC6	F	48	ND	ND	ND	ND	ND	26056	Yes	Negative
MC7	M	49	ND	ND	ND	ND	ND	7119	Yes	Negative
MC8	F	28	ND	ND	ND	ND	ND	2860	Yes	Negative
MC9	F	35	ND	ND	ND	ND	1960	ND	Yes	Positive
MC10	F	46	ND	ND	13015	ND	10646	ND	Yes	Positive
MC11	F	24	ND	ND	8922	ND	9369	ND	Yes	Positive
MC12	M	21	ND	ND	ND	ND	ND	ND	Yes	Negative
MC13	F	28	ND	ND	ND	ND	ND	ND	Yes	Negative
MC14	M	43	ND	ND	ND	ND	ND	ND	No	Negative
MC15	M	37	ND	ND	ND	ND	ND	1835	Yes	Negative
MC16	M	26	ND	ND	ND	ND	ND	ND	No	Negative
MC17	F	21	ND	ND	ND	ND	ND	ND	Yes	Positive
MC18	F	38	ND	ND	ND	ND	ND	ND	Yes	Positive
MC19	F	43	ND	ND	ND	ND	ND	ND	Yes	Positive
MC20	F	45	ND	ND	ND	ND	ND	ND	Yes	Positive
MC21	F	27	ND	ND	ND	ND	ND	ND	No	Negative
MC22	F	48	ND	ND	ND	ND	ND	23056	Yes	Negative
MC23	M	46	ND	ND	ND	ND	ND	ND	No	Negative
MC24	F	21	ND	ND	ND	ND	ND	8745	Yes	Negative
MC25	F	46	ND	ND	ND	ND	ND	4692	Yes	Negative
C1	M	40	ND	ND	ND	ND	ND	ND	Yes	Negative
C2	M	32	1030000	ND	978000	ND	1100000	ND	Yes	Negative
C3	F	19	ND	ND	ND	ND	ND	ND	Yes	Negative
C4	M	23	ND	ND	ND	ND	ND	ND	Yes	Negative
C5	M	26	ND	ND	ND	ND	ND	ND	No	Negative
C6	F	54	ND	ND	ND	ND	ND	ND	No	Negative
C7	M	29	ND	ND	ND	ND	ND	ND	No	Negative
C8	M	26	ND	ND	ND	ND	ND	ND	No	Negative
C9	F	29	1010000	ND	1010000	ND	1010000	ND	Yes	Negative
C10	F	46	ND	ND	ND	ND	ND	ND	No	Negative

**Table S2.** ME/CFS Serum Assay for Transferrable Antiviral Activity.

**RNA Virus (Influenza-A) Inhibition Assay.**

Serum Source	Inhibitory	Not Inhibitory	Totals
ME/CFS	9	1	10
Control	1	4	5
	10	5	15

ME/CFS Diagnostic Performance.

	Value	95% CI
p (Fisher's exact test)	0.017	n/a
Sensitivity	0.9	0.6-0.99
Specificity	0.8	0.38-0.99
Positive Predictive Value	0.9	0.6-0.99
Negative Predictive Value	0.8	0.38-0.99

Data from Figure 5A

**DNA Virus (HSV-1) Inhibition Assay.**

Serum Source	Inhibitory	Not Inhibitory	Totals
ME/CFS	10	0	10
Control	0	5	5
	10	5	15

ME/CFS Diagnostic Performance.

	Value	95% CI
p (Fisher's exact test)	0.0003	n/a
Sensitivity	1.0	0.72-1.0
Specificity	1.0	0.56-1.0
Positive Predictive Value	1.0	0.72-1.0
Negative Predictive Value	1.0	0.56-1.0

Data from Figure 5B